Effect of Shore A hardness and process parameters on the impact behaviour of SLA printed polymers

CHOUHAN, Ganesh, NAGWAL, Rita, BORADE, Himanshu, NAMDEO, Avinash Kumar, CHAUHAN, Shailendra Singh and BIDARE, Prveen

Discover Mechanical Engineering

RESEARCH Open Access

Effect of Shore A hardness and process parameters on the impact behaviour of SLA printed polymers

Ganesh Chouhan[1], Rita Nagwal[1], Himanshu Borade[1], Avinash Kumar Namdeo[2], Shailendra Singh Chauhan[3] and Prveen Bidare[4*]

*Correspondence:
Prveen Bidare
p.bidare@shu.ac.uk
[1]Department of Mechanical Engineering, Medi-caps University, Indore, Madhya Pradesh, India
[2]Department of Mechanical Engineering, Lingaya's Vidyapeeth, Faridabad, India
[3]Amity Institute of Technology, Amity University, Noida 201313, India
[4]School of Engineering and Built Environment, Sheffield Hallam University, Sheffield S1 1WB, UK

Abstract
Stereolithography (SLA) enables the fabrication of polymer components with exceptional dimensional accuracy; however, their resistance to impact loading is highly sensitive to material and processing parameters. In this study, the impact behaviour of SLA-printed polylactic acid (PLA) specimens was systematically investigated by evaluating the combined effects of Shore A hardness, layer height, and post-curing time. Specimens with hardness values of 50 A, 60 A, and 70 A were fabricated at layer heights of 20, 30, and 40 µm and subjected to post-curing durations of 30, 45, and 60 min. Charpy impact testing revealed that lower material hardness and finer layer resolution significantly enhance impact energy absorption, while extended post-curing improves interlayer bonding and fracture resistance. The highest impact performance was achieved at 50 A Shore hardness, 20 µm layer height, and 60 min of post-curing. In addition, fracture patterns indicated a semi-ductile failure mechanism characterized by progressive deformation and delayed crack propagation.

Keywords Impact performance, Shore A hardness, Post curing, Layer height, Additive manufacturing

1 Introduction

The role of resin composition, characteristics, and processing methods in relation to the mechanical properties of stereolithography-printed polymers is now much better recognized through recent advances in polymer research and additive manufacturing methods. In particular, the literature shows that proper resin proportioning, along with techniques such as hardness testing, is important for a high-performance material to exhibit consistent impact strength. There is a great degree of variation when reviewing SLA-printed polymers for their mechanical properties, according to some studies on SLA-printed components [1, 2].

Stereolithography (SLA), popularly known for its ability to produce accurate polymer parts [3] with a better surface finish compared to other additive methods of

manufacturing, has been employed for functional applications demanding a predefined mechanical specification [4]. In agreement with this notion, it has been stated by Liam et al. [5], that the tensile and flexural modulus of printed polymers by the SLA method are generally higher compared to FDM materials, but the impact resistance of the printed materials is inferior [5]. A study by Garcia et al. [6], established that graphene oxide was incorporated into a commercial-grade SLA resin with loadings of 0.2, 0.5, and 1% by weight, after which the printed specimens were subjected to mechanical testing regarding tensile, shear, and combined loading, with the resulting failure behaviour examined on the basis of the Drucker-Prager model [6].

The mechanical behaviour of SLA-printed polymers is strongly dependent on photopolymer resin formulation and homogeneity during mixing. Adjusted SLA resins include particulate reinforcements namely glass powder have been disclosed to represent concentrated tensile and compressive features as a result of optimize load transfer mechanisms [7]. As well, adding of metallic fillers into methacrylate-based photopolymers has represented advancement in shock resistance, highlighting the key part of material composition in energy absorption while dynamic loading [8]. Ahmad et al. (2024) finalized that the mechanical and viscoelastic properties of a commercial SLA resin were enhanced by the insertion of graphene nanoplatelets [9].

Many studies finalized that printing parameters like layer thickness, build orientation, and exposure conditions significantly influence the mechanical integrity of SLA-printed parts. Build orientation has been represent to affect anisotropy and fracture behavior, with horizontally oriented specimens often exhibiting higher strength and toughness than vertically printed counterparts [10]. Relative recognition from SLA, DLP, and LCD invention further represent that SLA prints basically exhibit higher level curved strength at optimized performance metric are implemented [11]. Wang et al.[12] indicate that inequality in build orientation towards printer axes notably effect of tensile, compressive, and flexural behavior of SLA-printed resins, marking the role of build angle in identifying mechanical performance [12]. Altarazi et al. (2022) examined the effects of print orientation and post-curing time on a 3D-printed denture base resin, indicating that vertical orientation enhanced mechanical behaviour, during curing beyond 30 min gave no advantages. According to Asim et al. [13], SLA process parameters such as build orientation and layer thickness significantly influence mechanical performance of biomedical raw materials, with vertical orientation improving tensile, flexural, and impact strength. Regression model was also invented to communicate these characteristics to the printing conditions [13]. Oliveira et al. [14] estimate the result of post-curing time and printing direction on the mechanical behaviour of water-washable SLA resins, using experimental tests and numerical modeling to enhance material characteristics [14].

The Tensile, flexural, and impact examination are extensively preferred in mechanical evaluation of SLA-printed polymers to evaluate structural dependability. As a result of these variables control crack initiation and energy dissipation mechanisms, impact performance is especially sensitive to crosslink density, print orientation, along with post-curing conditions [15]. Functional polymer components study has also indicate that conditioning and subjection to the environment might affect impact resistance, highlighting necessity of controlled testing environment [8]. This study found that whereas traditional and milling specimens showed no discernible strength changes, thermal cycling significantly reduced flexural and impact strength as well as Weibull reliability

in 3D-printed samples. After thermal exposure, hardness rose in conventional materials but fell in milled and 3D-printed groups. Cheadle et al. [16] evaluated the effect of orientation and post-curing on mechanical properties (tensile and flexural) of SLA resin, highlighting how process factors influence mechanical strength [16].

Shore A hardness is basically experienced to characterize the elastic hardness of polymeric and elastomeric materials and has been shown to highly influence their mechanical output [17]. Last research finalized that Shore A values range from very soft elastomers (≈ 20–30 Shore A) to semi-rigid polymers (≈ 90–100 Shore A), covering exercise from sealing and damping to load-bearing parts [18]. It has been demonstrated that higher Shore A hardness has better wear resistant qualities, tensile strength, and indentation resistance [19]. Conversely, hardness adversely affects material elasticity, specifically the material's elongation at fracture, due to increased stiffness resulting from restricted elastomeric chain motion. Although increased Shore A hardness is a desirable material property for structural integrity, research by Reff (2010) indicates that it causes an increase in the elastic modulus properties due to material stiffness [20]; on the other hand, material hardness can negatively impact material fatigue properties, especially for materials under constant cyclic loading [21]. However, the correlation between Shore A hardness and the mechanical attribute is affected by the level of crosslink density, filler, and curing steps, thereby reflecting that the level of hardness is unable to accurately determine the mechanical property in the absence of the material composition [22]. Thus, the influence of Shore A hardness on the mechanical properties is crucial in identifying the optimization of enhanced polymer materials in the mechanical engineering field, which requires the interaction of hardness and flexibility [23].

The suggested work aims to generate samples with varying hardness levels by utilizing machine variables and post-processing time for lightweight impact applications. This study aims to fabricate SLA-printed specimens and investigate the effect of key processing parameters on their impact performance, with additional comparison to pure PLA material.

2 Materials and methods

This section outlines a discussion on the criteria for choosing materials, process variables, manufacturing method, post-processing of three-dimensional printing samples, and testing method. In this research work, there were three types of PLA photopolymers with varying Shore hardness values (50 A, 60 A, and 70 A) and three layers with heights (20, 30, and 40 μm), along with three post-curing times (30 min, 45 min, and 60 min) to examine in a combined manner the individual effects on impact behavior of stereolithography SLA. Figure 1 shows how work is performed with a flow process on a priority basis right from material selection to testing of samples.

2.1 Material selection and additive manufacturing

Three PLA-based photopolymer resins with distinct Shore A hardness values of 50 A, 60 A, and 70 A were selected to systematically investigate the effect of material hardness on the impact performance of stereolithography (SLA) additively manufactured components. These materials were procured from Siraya Tech, USA, and represent a broad range of elastomeric to semi-rigid behaviour within the PLA resin family. The selected hardness range enables a comprehensive evaluation of the relationship between

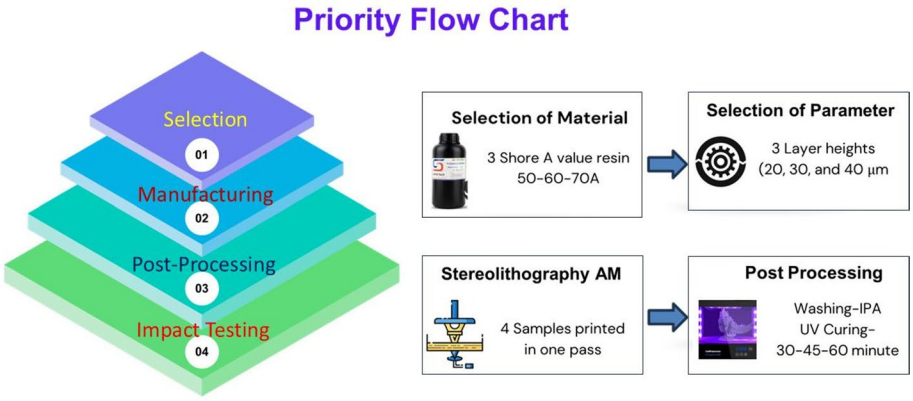

Fig. 1 Targeted Work flow for SLA manufactured impact samples

resin flexibility, energy absorption capacity, and fracture response under impact loading. Standardized impact test specimens were fabricated using a stereolithography process, ensuring consistent processing conditions to isolate the influence of Shore hardness on mechanical performance.

In this study, CAD models of lattice samples were designed using nTopology software. To obtain the gcodes, the planned model is saved in stl format and imported into the slicer program Halot Box (Creality). Moreover, the software gives the weight of the sample, total cost, printing duration, and material used. Before giving the print command to the SLA 3D printer, several pre-processing steps were carried out to reduce the chances of failure of the samples. During the pre-processing stage, the first step was the orientation of the sample in the machine platform, whether vertical, horizontal, or inclined. In our research, horizontal build orientation is used. The build orientation can be responsible for layer adhesion, accuracy in terms of dimension, and anisotropy of the printed sample. The second step carried out in pre-processing is cleaning and levelling of the build platform. Filtration of resin to remove particles and appropriate tensioning of FEP film.

Creality HALOT Mage S 14 K SLA Printer is used to print the specimen, where the maximum printing range of $8.78 \times 4.96 \times 9.06$ inches, printing speed of 150 mm/h, and maximum resolution for surface polish are used. Siraya Tech FAST ABS-Like 3D Printer Resin 405 nm UV-Curing is the parent material Providing the non-brittle high precision, low volume shrinkage, high tensile strength, and suitable modus of elasticity. Tensile strength and elastic modulus of the material is 32-52 MPa, and 1.0 to 2.65GPa respectively. Density of the resin is 1.05–1.25 g/cm^3, shrinkage is around 3.72–4.24%, EBG (Electromagnetic Band-gap) varies highly from 3.0% to 150%, depending upon the testing process, and melting temperature of the resin ranges around 150°-162 °C. G-code input is used in the process where four samples are prepared at one time. The total time to print the four samples is 37 min, requiring 201 layers for completion. The printed samples did not utilize the support system during the printing process. The machine has maximum printing resolution of ultra-high 14 K (16.8×24.8 µm). Three PLA-based resins with varying Shore A hardness values were utilized as the base materials for the experimental investigation. Nine impact specimens were fabricated for each Shore A hardness level (50 A, 60 A, and 70 A) of PLA resin, yielding a total of 27 samples.

Following sample printing, post-processing was used to remove, clean, and cure the samples in order to obtain the necessary dimensional accuracy, mechanical impact performance qualities, minimizes flaws, premature failure, and enhances surface finish. At first, the printed parts are meticulously removed off the build platform with a scraper. Avoid distortion or damage, particularly for fragile or thin-walled components. The extracted samples were subsequently cleaned with isopropyl alcohol in automated washing stations. Appropriate washing duration is upheld to avert surface tackiness or swelling. Washed components are air-dried, followed by UV curing to finalize the polymerization of the printed resin (see Fig. 2). This study examines the efficacy of three curative durations: 30, 45, and 60 min.

2.2 Charpy impact testing

Charpy pendulum impact testing was carried out using a Tinius Olsen impact testing machine (Easton Road, Horsham, PA 19044, USA) to evaluate the impact energy absorption of the SLA-manufactured samples (see Fig. 3a). The pendulum impact tester is a versatile and reliable instrument designed to measure the energy absorbed by materials during fracture and fully complies with ASTM E23, EN 10045-2, and ISO 148 standards [24]. The tests were conducted using a basic pendulum with a maximum energy capacity of 406 J, a drop height of 1.052 m, and an impact velocity of 5.47 m/s. The overall machine dimensions were 2108 × 508 × 1854 mm, with a gross weight of 736 kg. Rectangular specimens were prepared in accordance with the specified standard, with dimensions of 10 × 10 × 55 mm^3 and a 45° V-notch geometry. Figure 3b shows the standard mechanism used to clamp the sample in test machine. Additionally, the impact tests were conducted at room temperature using a pendulum impact testing machine that was calibrated to apply a specific impact force to the specimen. Furthermore, the impact strength of the specimen was determined based on the impact absorbed energy and the cross-sectional area of the specimen. Upon conducting the impact testing of the specimen, the deformation and fracture occurred in the specimen around the notch section as shown in Fig. 3c.

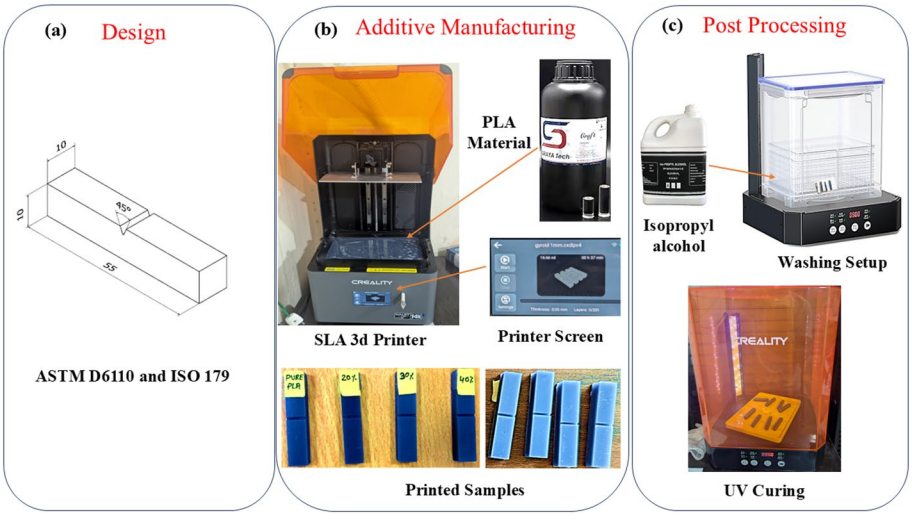

Fig. 2 Illustration of work from design to development, (**a**) Adopted standard for impact sample, (**b**) Stereolithography additive manufacturing technique for printing the samples, and (**c**) Applied post processing

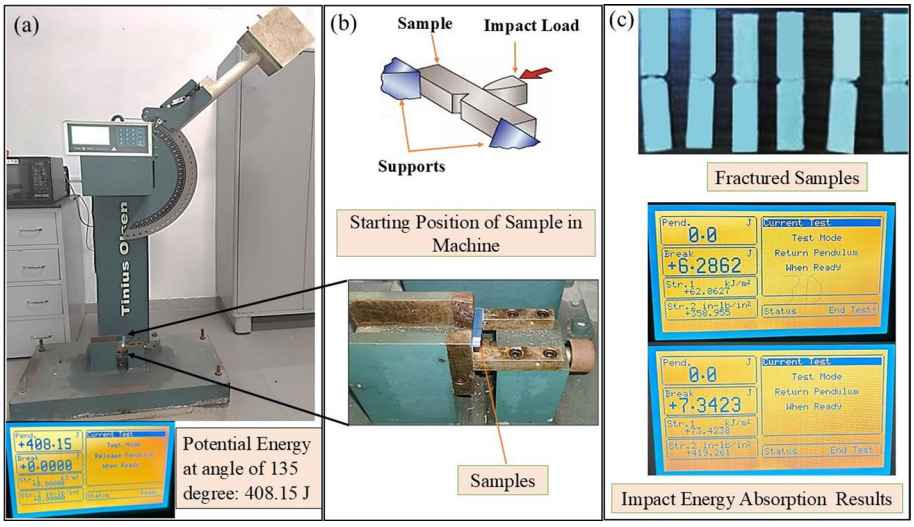

Fig. 3 Schematic representation of impact testing, (**a**) Charpy testing setup, (**b**) mechanism to clamp sample, and (**c**) initial stage potential energy with fractured samples

Table 1 Factors and levels for manufacturing the impact samples

Control factor	Level 1	Level 2	Level 3
Shore A value (%)	50	60	70
Layer height (μm)	20	30	40
Curing time (min)	30	45	60

2.3 Determination of Taguchi method

This research employed the Taguchi experimental design method utilizing the L27 3^3 orthogonal array matrix, which comprises 27 experiments with three factors, each at three levels. The full factorial Taguchi experimental design was implemented to minimize the number of trials, reduce costs, and attain optimal results in a shorter timeframe. The Taguchi method offers a systematic and efficient approach for optimizing system parameter designs with significantly less impact than conventional optimization techniques necessitate. As indicated in Table 1, the outcomes of SLA 3D printed impact test samples will be influenced by three control factors and three levels of each factor: Shore A value is the first factor, layer height is the second, and curing time is the third (Table 2).

3 Results and discussion

This study attempts to quantitatively evaluate the impact performance of SLA-fabricated specimens by systematically examining the influences of Shore A hardness, layer height, and post-curing duration on impact energy absorption during fracture. A systematic experimental approach was utilized to assess the individual and interactive effects of Shore hardness and curing duration. The relationship between hardness-layer height and layer height-curing time on the fracture behaviour of specimens subjected to Charpy impact loading. The experimental results from the 27 studies assessed through impact testing are presented in Table 3.

The Charpy impact test results demonstrate a clear enhancement in impact energy absorption with increasing incorporation of lower Shore hardness PLA into the base PLA matrix (see Fig. 4a). Relative to pure PLA, the absorbed impact energy increased

Table 2 Design matrix of orthogonal array $L27^3$ for the experimental runs

Trial number	Shore A value (%)	Layer height	Curing time
1	1	1	2
2	1	1	2
3	1	1	2
4	1	2	1
5	1	2	1
6	1	2	1
7	1	3	3
8	1	3	3
9	1	3	3
10	2	1	1
11	2	1	1
12	2	1	1
13	2	2	3
14	2	2	3
15	2	2	3
16	2	3	2
17	2	3	2
18	2	3	2
19	3	1	3
20	3	1	3
21	3	1	3
22	3	2	2
23	3	2	2
24	3	2	2
25	3	3	1
26	3	3	1
27	3	3	1

marginally by approximately 1.37% for the 20% mixed sample, indicating a limited toughening effect at low modification levels. However, a relatively significant improvement of 23.36% was seen in the case of the 30% mixed specimen, indicating effective stress distribution and energy absorption during fracture. The largest elevation of 44.10% was seen in the case of the 40% mixed specimen compared to that of pure PLA, clearly indicating significant improvements in the toughness and strain ability of the samples before fracture. It is clear from the above observations that increasing the content of low Shore hardness samples tends to ensure effective improvements in impact resistance properties by lowering brittleness and increased resistance to crack propagation in SLA-produced PLA samples.

3.1 Effects of Shore A value, layer height, and curing time

The Shore A hardness has a major effect on the impact behaviour of the fabricated specimens *(*see Fig. 4b). As the Shore A value rises from 50 A to 70 A, there is a steady decrease in impact strength, with 50 A showing the highest mean impact strength. Because harder materials are stiffer and have a lower capacity to absorb energy under impact loading, this trend supports the negative impact performance impact of rising hardness. Experimental specimens with a Shore hardness of 50 A demonstrated consistently superior impact performance, with impact strength values between 56.92 and 73.42 kJ/m² and a maximum energy absorption of 7.342 J, correlating to an impact strength of 73.42 kJ/m², signifying improved energy dissipation capacity. Conversely,

Table 3 Impact performance of SLA 3d printed samples according to runs

Run	Input parameters			Output parameters	
	A: Shore A	B: Layer Height (μm)	C: Curing Time (min)	Impact Energy Absorption (J)	Impact Strength (KJ/m^2)
1	50 A	20	30	6.113	61.13
2	50 A	20	45	6.865	68.65
3	50 A	20	60	7.342	73.42
4	50 A	30	30	5.823	58.23
5	50 A	30	45	6.396	63.96
6	50 A	30	60	6.908	69.08
7	50 A	40	30	5.692	56.92
8	50 A	40	45	5.911	59.11
9	50 A	40	60	6.661	66.61
10	60 A	20	30	6.019	60.19
11	60 A	20	45	6.635	66.35
12	60 A	20	60	6.833	68.33
13	60 A	30	30	5.702	57.02
14	60 A	30	45	6.199	61.99
15	60 A	30	60	6.701	67.01
16	60 A	40	30	5.611	56.11
17	60 A	40	45	5.718	57.18
18	60 A	40	60	6.588	65.88
19	70 A	20	30	5.713	57.13
20	70 A	20	45	6.335	63.35
21	70 A	20	60	6.502	65.02
22	70 A	30	30	5.593	55.93
23	70 A	30	45	6.188	61.88
24	70 A	30	60	6.448	64.48
25	70 A	40	30	5.379	53.79
26	70 A	40	45	5.922	59.22
27	70 A	40	60	6.401	64.01

specimens exhibiting elevated Shore hardness (50 A and 70 A) shown a gradual decline in impact strength, with average values diminishing from roughly 64.1 kJ/m^2 at 50 A to 60.5 kJ/m^2 at 70 A. The decrease is ascribed to heightened material stiffness and diminished molecular chain mobility in more rigid materials, which constrains plastic deformation and limits energy absorption during impact loading.

Layer height had a significant effect on the impact behaviour of the specimens (see Fig. 4c); lower layer heights consistently produced higher impact energy absorption and impact strength for all combinations of Shore A hardness and curing time. The highest average impact strength of ~ 64.8 kJ/m^2 was recorded for specimens fabricated at 20 μm layer height, while increasing the layer height to 30 μm and 40 μm resulted in a gradual deterioration of the impact performance characterized by a reduction of the average impact strength to about 62.2 kJ/m^2 and 59.9 kJ/m^2, respectively. For instance, at 50 A Shore hardness and a curing time of 60 min, the impact energy decreased from 7.342 J at 20 μm to 6.661 J at 40 μm. This is explained by poorer interlayer bonding and increased populations of interfacial voids at higher layer heights, which act as stress concentrators and promote crack initiation during impact loading [25].

The significant positive correlation between the curing time and impact performance is evident. Increasing the curing time from 30 min to 60 min showed a constant enhancement in terms of both impact energy absorption capacity and impact strength

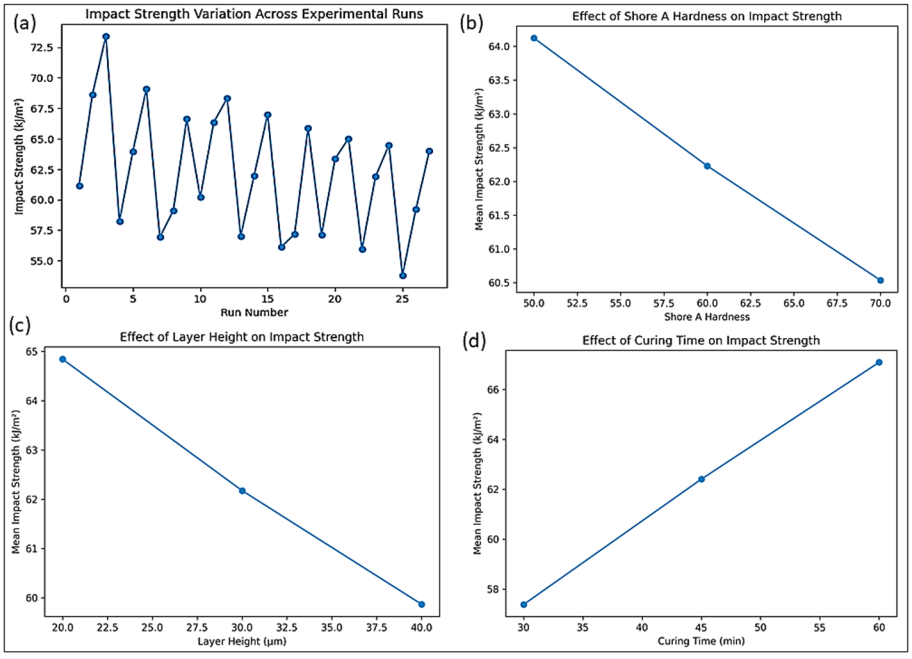

Fig. 4 Impact test results for all SLA printed samples and effect of Shore A value, layer height, and curing time

for all Shore A hardness and layer height combinations (see Fig. 4d). The average impact strength increased from approximately 57.4 kJ/m² for 30 min to 62.4 kJ/m² for 45 min, denoting a rise of about 8.7%, and further increased to 67.1 kJ/m² for 60 min, indicating a total increase of 16.9% compared to the 30-minute curing time. This can be attributed to the high cross-link density and increased interlayer adhesiveness, contributing to high resistance to sudden impact loading conditions. For Shore hardness 60 A and a layer height of 30 μm, the impact energy increased from 5.702 J for 30 min to 6.701 J for 60 min, denoting a rise of about 17.5%. Alongside, the impact strength increased from 57.02 kJ/m² to 67.01 kJ/m², denoting an increase of 17.5%.

3.2 Combine effects of Shore A value, layer height, and curing time

The Charpy impact test results for pure PLA and PLA-based materials with varying Shore hardness values (50, 60, 70, and 80 Shore A) are summarized in terms of total energy absorbed. Pure PLA exhibited an impact energy absorption of 5.0960 J. With the incorporation of softer Shore A materials, a gradual increase in impact energy was observed. The sample containing 20% Shore-modified PLA absorbed 5.1658 J, indicating a marginal improvement over pure PLA. A more pronounced enhancement was recorded for the 30% mix, which absorbed 6.2862 J, while the 40% mix demonstrated the highest impact resistance with an absorbed energy of 7.3423 J. The results indicate that increasing the proportion of lower Shore hardness material significantly improves the impact energy absorption capability of PLA, suggesting enhanced toughness due to improved energy dissipation during fracture.

3.2.1 Combine effects due to Shore A hardness and curing time

Figure 5a shows that the samples' energy absorption varied significantly, from about 5.3 J to 7.34 J, according to the findings of the impact tests. Sample 3 had the greatest impact energy absorption (≈7.34 J), which indicates that it is very good at dissipating energy,

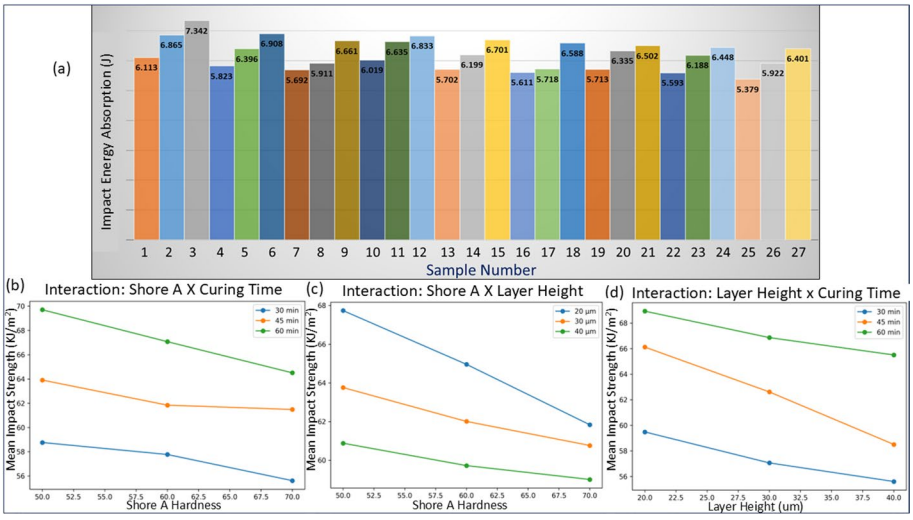

Fig. 5 **a** Impact resistant/Energy absorbed by the samples during fracture, **b** Combine effect of Shore A value and curing time, **c** Combine effect of Shore A value and layer height, and **d** Combine effect of layer height and curing time

whereas samples like 25 had lower values (≈ 5.38 J), which means that they are significantly less resistant to impact.

The Fig. 5b clearly demonstrates a strong synergistic interaction between Shore A hardness and curing time; at a Shore hardness of 50 A, extending the curing duration from 30 min to 60 min elevated the mean impact strength from roughly 58.8 kJ/m² to 69.7 kJ/m², representing improvement of relatively 18.6%. This propose that softer materials derive the highest advantage from prolonged curing, resulting in greater cross-linking and superior energy dissipation capacity. towards Shore hardness of 60 A, a comparable movement was noted, with impact strength rising from around 57.8 kJ/m² to 67.1 kJ/m², reflecting enhancement of almost 16.1% when the curing time was increased from 30 min to 60 min. Correspondingly, for 70 A Shore hardness, Shock resistance rose from roughly 55.6 kJ/m² to 64.5 kJ/m², amending in an enhancement of generally 16.0%. To summarize, the highest impact strength was collected at 50 A hardness with 60 min of curing, as the lowest results was seen at 70 A hardness with 30 min of curing. Finally, fluctuation between these two utmost circumstances was across 25.3%, representing that prolonged curing duration can somewhat mitigate the negative consequences of heightened Shore A hardness impact, evidenced by the notable enhancement in impact strength with prolonged curing time.

3.2.2 Combine effects due to Shore A hardness and layer height

The Fig. 5c depicting connection between Shore A hardness and layer demonstrates a persistent, virtually parallel decline, giving opinion that while both elements substantially affect impact strength, their interaction effect is lesser. throughout layer heights, impact strength diminishes like Shore A hardness escalates from 50 A to 70 A. Specimens produced at a reduced layer height of 20 µm frequently indicate superior impact strength similar to those produced at 30 µm and 40 µm throughout every hardness levels. Peak mean impact strength is listed at a 50 A Shore hardness and a 20 µm layer height, whereas the lowest values are found at 70 A and 40 µm, endorsement the significant adverse impacts of material rigidity and interlayer lack of consistency.

3.2.3 Combine effects due to layer height and curing time

The presence of a strong influence on the impact performance from the Fig. 5d, the plot of layer height and curing time, is evident from the differences in the patterns of the interaction plot and the % variation in the impact strength. While the average impact strength decreased from about 59.5 kJ/m² at a layer height of 20 μm to 55.6 kJ/m² at a height of 40 μm in a 30-minute curing process, it shows a variation of about 6.6%, where the impact strength decreased with the reduced curing times due to the poor interlayer adhesion.

On the other hand, when the curing time took 45 min, there was a decrease in the value of impact strength from around 66.1 kJ/m² for a layer thickness of 20 μm to 58.5 kJ/m² for a layer thickness of 40 μm, indicating a decrease of approximately 11.5%, thus again establishing the synergistic effect due to increased height and Significantly, at a curing time of 60 min, the reduction in impact strength with the increment in layer height was remarkably mitigated. The impact strength dropped slightly from approximately 68.9 kJ/m² for the 20 μm layer height to 65.5 kJ/m² at the 40 μm layer height, reflecting merely a slight reduction of about 4.9%. This clearly shows that the longer curing time enhances the adhesion between the layers and counters the adverse effects associated with larger printed layers. Ultimately, the Percentage Test confirms that the longer curing times significantly reduce the impact strength dependency on the increased height of the layers, while improper curing exacerbates the negative impact of increased thickness.

3.3 Relative improvement over pure PLA material

The optimized SLA-manufactured samples performed significantly better in terms of impact performance compared to the pure PLA material. The maximum absorbed energy of 7.342 J recorded under the conditions of 50 A Shore hardness, 20 μm layer height, and 60 min of curing was almost 44.1% higher compared to pure PLA, whose absorbed energy is 5.096 J. The impact strength of 73.42 kJ/m² reflects a value increase of approximately 44.1% with respect to the pure PLA impact strength of 50.96 kJ/m². Based on the high value increase, it has been confirmed that regulated hardness and refined layer production, plus sufficient post-curing, greatly enhance the energy dissipation capacity. The fracture response shifted from brittle behaviour in pure PLA to a semi-ductile mode in the optimized specimens, signifying enhanced molecular mobility and increased interlayer adhesion under Charpy impact loading.

4 Conclusion

In this study, attention is devoted to the preparation and assessment of the impact performance of charpy impact specimens made by resins containing different hardness values of thermosetting PLA. The thermosetting PLA resins with Shore A hardness ranging from 50 A to 80 A were prepared by SLA-based additive manufacturing. Key processing parameters, including layer thicknesses of 20, 30, and 40 μm and post-curing times of 30, 45, and 60 min, were systematically varied. Charpy impact tests were conducted to investigate the influence of PLA Shore A hardness and processing parameters on impact performance, with particular emphasis on applications related to automotive headlight and taillight housing com ponents.

- The findings from the experiment indicated that curing time had the most significant beneficial effect, followed by layer height, however hardness negatively impacted impact performance.
- The most effective impact performance was attained at 50 A shore hardness, 20 μm layer height, and 60 min of curing time.
- Impact strength increased by 44.1%, from 50.96 kJ/m² for pure PLA to 73.42 kJ/m² for optimized SLA material, demonstrating superior resistance to sudden loading.
- Fracture characteristics indicated a semi-ductile failure mode in optimized specimens, whereas pure PLA is dominated by brittle behavior with limited energy dissipation.
- The material is appropriate for lightweight structural or functional applications due to its demonstrated moderate toughness and sufficient resistance to quick impact loads.

Acknowledgements
For open access, the author has applied a Creative Commons Attribution (CC BY) license to any Author Accepted Manuscript version arising from this submission."

Author contributions
Ganesh Chouhan: Writing—Original Draft, Rita Nagwal- Methodology, Investigation Himanshu Borade- Data curation, Avinash Kumar Namdeo- Formal analysis, Shailendra Singh Chauhan- Validation, Prveen Bidare-Writing—Review & Editing, Supervision.

Funding
This is not applicable.

Data availability
On request, the corresponding authors will provide all information and materials necessary to produce the findings in this study.

Declarations

Ethical approval
This study does not involve human participants or animals. Therefore, ethical approval was not required.

Competing interests
The authors declare no competing interests.

Consent to participate
Not applicable.

Consent for publication
Not applicable.

Received: 12 February 2026 / Accepted: 29 April 2026
Published online: 11 June 2026

References

1. Dias Gonçalves VP, Vieira CM, Simonassi NT, et al. Evaluation of Mechanical Properties of ABS-like Resin for Stereolithography Versus ABS for Fused Deposition Modeling in Three-Dimensional Printing Applications for Odontology. Polym (Basel). 2024;16:2921.
2. Husna A, Ashrafi S, Tomal ANMA, et al. Recent advancements in stereolithography (SLA) and their optimization of process parameters for sustainable manufacturing. Hybrid Adv. 2024;7:100307. https://doi.org/10.1016/j.hybadv.2024.100307.
3. Afridi A, Al Rashid A, Koç M. Recent advances in the development of stereolithography-based additive manufacturing processes: A review of applications and challenges. Bioprinting. 2024;43:e00360. https://doi.org/10.1016/j.bprint.2024.e00360.
4. Al Rashid A, Ahmed W, Khalid MY, Koç M. Vat photopolymerization of polymers and polymer composites: Processes and applications. Addit Manuf. 2021;47:102279. https://doi.org/10.1016/j.addma.2021.102279.
5. O'Connor Liam. Comparative analysis of the mechanical properties of FDM and SLA 3D printed components. J Micromanufacturing. 2025;25165984251364690. https://doi.org/10.1177/25165984251364689.
6. Garcia GE, de Sousa Junior RR, Gouveia JR, dos Santos DJ. Graphene Oxide-Based Nanocomposites for Stereolithography (SLA) 3D Printing: Comprehensive Mechanical Characterization under Combined Loading Modes. Polym (Basel). 2024;16:1261.
7. Susanto B, Putro AJ, Ristyawan MR, et al. Enhanced Mechanical Properties of the Additively Manufactured Modified Hybrid Stereolithography (SLA)–Glass Powder. J Compos Sci. 2025;9:205.

8. Stark BL, Gamboa M, Esparza A, et al. Materials Characterization of Stereolithography 3D Printed Polymer to Develop a Self-Driven Microfluidic Device for Bioanalytical Applications. ACS Appl Bio Mater. 2024;7:7883–94. https://doi.org/10.1021/acsabm.4c00059.
9. Ahmad KH, Mohamad Z, Khan ZI. Influence of Graphene Nanoplatelets and Post-Curing Conditions on the Mechanical and Viscoelastic Properties of Stereolithography 3D-Printed Nanocomposites. Polym (Basel). 2024;16:2721.
10. Martínez Raya A, Aranda-Ruiz J, Sal-Anglada G, et al Effect of Printing Orientation on the Mechanical Properties of Low-Force Stereolithography-Manufactured Durable Resin. Appl Sci. 2024;14(20):9529. https://doi.org/10.3390/app14209529.
11. Katheng A, Prawatvatchara W, Chaiamornsup P, et al. Comparison of mechanical properties of different 3D printing technologies. Sci Rep. 2025;15:18998. https://doi.org/10.1038/s41598-025-03632-1.
12. Wang E, Yang F, Shen X, et al. Investigation and Optimization of the Impact of Printing Orientation on Mechanical Properties of Resin Sample in the Low-Force Stereolithography Additive Manufacturing. Mater (Basel). 2022;15. https://doi.org/10.3390/ma15196743.
13. Asim M, Butt SI, Haq MR, Jan D. (2025) Optimization of 3D Printing Parameters for Enhanced Mechanical Strength Using Taguchi Method. Eng. Proc. 111(1):26.
14. Oliveira GC, Oliveira VA, Pinto CC, et al. Influence of Post-Curing Time and Print Orientation on the Mechanical Behavior of Photosensitive Resins in mSLA 3D Printing. Appl Mech. 2025;6:71.
15. Saunders J, Lißner M, Townsend D, et al. Impact behaviour of 3D printed cellular structures for mouthguard applications. Sci Rep. 2022;12:4020. https://doi.org/10.1038/s41598-022-08018-1.
16. Cheadle AMG, Maier E, Palin WM, et al. The impact of modifying 3D printing parameters on mechanical strength and physical properties in vat photopolymerisation. Sci Rep. 2025;15:12592. https://doi.org/10.1038/s41598-025-97294-8.
17. Dasaesamoh A, Khotmungkhun K, Subannajui K. Natural Rigid and Hard Plastic Fabricated from Elastomeric Degradation of Natural Rubber Composite with Ultra-High Magnesium Carbonate Content. Polym (Basel). 2023;15:3078.
18. Gent AN. Engineering with Rubber: How to Design Rubber Components. Hanser; 2012.
19. Chatzistergos P, Allan D, Chockalingam N, Naemi R. Shore hardness is a more representative measurement of bulk tissue biomechanics than of skin biomechanics. Med Eng Phys. 2022;105:103816. https://doi.org/10.1016/j.medengphy.2022.103816.
20. Reff B. (2010) 14 - Noise and vibration refinement of chassis and suspension. In: Wang XBT-VN and VR, editor. Woodhead Publishing, pp 318–350.
21. Pieniak D, Jedut R, Gil L, et al. Comparative Evaluation of the Tribological Properties of Polymer Materials with Similar Shore Hardness Working in Metal–Polymer Friction Systems. Mater (Basel). 2023;16:573.
22. Liao Z, Hossain M, Yao X. Ecoflex polymer of different Shore hardnesses: Experimental investigations and constitutive modelling. Mech Mater. 2020;144:103366. https://doi.org/10.1016/j.mechmat.2020.103366.
23. Wang B, Li X, Peng X, et al. Influence of Nitrile Butadiene Rubber (NBR) Shore Hardness and Polytetrafluoroethylene (PTFE) Elastic Modulus on the Sealing Characteristics of Step Rod Seals. Lubricants. 2023;11:367.
24. Lucon E, Splett J. Effect of Charpy Striker Configuration on Low- and High-Energy. NIST Verification Specimens. 2018;123:1–13.
25. Candau N, Fernández Navarrete A, Lara Casanova G, et al. Control by the curing time of the strain induced crystallization and elastocaloric properties in natural rubber and natural/waste rubber blends. Polym (Guildf). 2024;312:127628. https://doi.org/10.1016/j.polymer.2024.127628.

Publisher's note